# Design and Evaluation of the Grid-Connected Solar Power System at the Stage of DC BUS with Optimization of Modulation Frequency for Performance Improvement

Nguyen Duc Minh[1(✉)], Quach Duc-Cuong[2], Nguyen Quang Ninh[1], Y Nhu Do[3], and Trinh Trong Chuong[2]

[1] Institute of Energy Science, Vietnam Academy of Science and Technology, Cau Giay, Vietnam
minhnguyenduc.ies@gmail.com
[2] Hanoi University of Industry, Hanoi, Vietnam
[3] Hanoi University of Mining and Geology, Hanoi, Vietnam

**Abstract.** In grid-connected solar panel systems, the power converters play a very im-portant role in control systems, because the characteristics of solar panel system are that the generation power is constantly changing due to dependence on weath-er conditions. This article presents the research results of the application of power electronic converter in grid-connected solar power system. In particular, we focus on building an algorithm to control and simulate the grid-connected solar power system at the DC-BUS stage by setting an optimal set of SVPWM (Space Vector Pulse Width Modulation) modulation frequencies when the pulse width values are different. The simulation results on Matlab/Simulink show that the system op-erates stably, ensures the requirements of DC-BUS grid integration. The set-up system operates safely, has a simple control structure and algorithm, is easy to calibrate and makes it ready for practical applications.

**Keywords:** Maximum power point tracking · Space Vector Pulse Width Modulation · Incremental conductance · Grid-connected solar power system

## 1 Introduction

The power converters are commonly used in distributed energy sources: wind power, solar power, … and play a very important role in control systems [1]. In a solar panel system, the commonly used DC/DC converter is the implementation mechanism of the MPPT maximum power sticking algorithm of the solar panel array. MPPT uses a DC/DC converter to adjust the input voltage from the solar panel, convert it and provide the load so that the output from the solar panel is maximum. However, the use of a DC/DC converter can increase the power loss in the system [2] and may lead to a reduction in the energy conversion performance of the entire solar power system. This raises the increase of DC/DC converter's conversion performance. In fact, the performance of the DC/DC


N.-S. Vo and V.-P. Hoang (Eds.): INISCOM 2020, LNICST 334, pp. 270–288, 2020.
https://doi.org/10.1007/978-3-030-63083-6_21

converter is not constant, but rather depends on the power transmitted through it [3]. Typically, the performance of the DC/DC converter reaches its maximum value within 50%–60% of the design power and decreases rapidly if the power through it becomes smaller [4]. However, in solar panels, the output power is not fixed, the power reaches the rated value at the time of noon and the output power is small in the morning and afternoon [5], the period in which the power is smaller than 40% can reach several hours a day, not to mention shade and sunny days. Thus, in this case, the power through the DC/DC converter will be quite small (less than 40%), therefore, the performance of the DC/DC converter is very low and most of the power is consumed in the converter. Therefore, the design of a high-performance DC/DC converter is essential. Many authors have proposed the structure of DC/DC units with high performance [6–8]. Several other studies have suggested solutions to reduce the loss in the converter to improve the performance [9, 10]. However, its performance still depends on the power passing through it. That means that, during the period when the solar panel output power is very low, the DC/DC converter performance is still very low and there is not a reliable enough dataset in a sufficient range of the modulation frequencies to determine the relationship between the hashing frequency and the modulation pulse width to the performance of the DC/DC Boost unit.

This article presents the research results of the application of power electronic converter in grid-connected solar power system. In particular, we focus on building a algorithm to control and simulate the grid-connected solar power system at the DC-BUS stage by setting an optimal set of SVPWM modulation frequencies when the control value is different (width D is different). The simulation results on Matlab/Simulink show that the system operates stably, ensures the requirements of DC-BUS-side grid integration.

## 2 Structure of Power Blocks in the System

Figure 1 illustrates the structure of the system integrated into the solar power source. The DC voltage from solar power sources is usually low voltage, therefore, step-up DC/DC converters are necessary. Meanwhile, the grid power source is the AC power source with fixed frequency and amplitude. The DC bus power is directly supplied to local DC loads. From the DC bus, through the DC voltage inverter, it changes to AC at the AC bus. The power at the AC bus is fed to the AC load and connected to the grid through

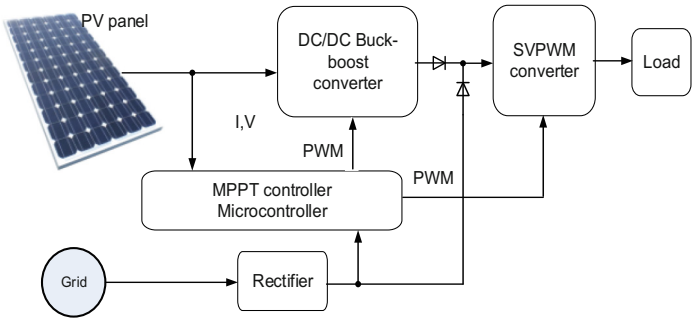


**Fig. 1.** Block structure of the system.

the transformer. Currently, the inverter technology to generate sinusoidal voltage mainly uses SVPWM modulation technology.

### 2.1 Boost DC/DC Block

The DC/DC converters are usually divided into 2 types with isolation and non-isolation. The isolation type uses small size high frequency electrically isolated transformer to isolate the input DC power from the DC output power supply and to increase or decrease the voltage by adjusting the transformer factor. This type is often used for DC power supplies using electronic keys. The most common is the bridge, half bridge and flyback circuits. In fact, many grid-working systems often use electrically isolated types for many safety reasons. Non-isolated DC/DC type do not use the isolation transformer. Common types of DC/DC converters used in PV systems include:

– Buck unit
– Boost unit
– Buck-boost unit

The selection of which type of DC/DC to use in the PV system depends on the system requirements and the load on the output voltage of the solar panel array [11–13]. The Buck unit is able to determine the optimum power operating point whenever the input voltage exceeds the output voltage of the converter, which is less likely when the radiation intensity of the light is low. The Boost unit can set the optimal working point even with low light intensity. The system that works with the grid uses the Boost unit to increase the output voltage for the load before putting it into the DC/AC converter. If the pulse hash frequency of the DC/DC voltage hashing stage is sufficient, and the system operates in continuous current mode (relating to parameters such as modulation pulse width, modulation frequency, inductance and capacitance of the DC/DC stage), the Boost DC/DC unit model on Fig. 2 in dynamic mode is described by Eq. (1) [14].

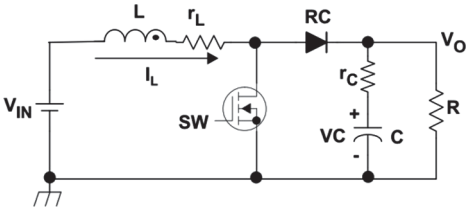


**Fig. 2.** Boost DC/DC circuit diagram

$$G_{dv}(s) = \frac{\hat{V}(s)}{\hat{D}(s)} \approx G_{d0} \frac{(1 + r_c Cs)\left(1 - \frac{L}{R}\left(\frac{V_0}{V_{IN}}\right)^2 s\right)}{\frac{1}{\omega_0^2}s^2 + \frac{1}{\omega_0 Q}s + 1} \quad (1)$$

In which:
$G_{dv}(s)$ is the transfer function of the Boost unit;
$\hat{V}(s)$ is the Laplace image of the output voltage;
$\hat{D}(s)$ is the Laplace image of the control signal which is the modulation pulse width;
$G_{do}$ is a transfer function in a set mode, calculated by:

$$G_{d0} = \frac{V_{IN}}{(1-D)^2} = \frac{V_O^2}{V_{IN}} \tag{2}$$

Frequency:

$$\omega_0 \approx \frac{1}{\sqrt{LC}}\sqrt{\frac{r_L + 1 - D^2R}{R}} \approx \frac{1}{\sqrt{LC}}.\frac{V_{IN}}{V_0} \tag{3}$$

and:

$$Q \approx \frac{\omega_0}{\frac{r_L}{L} + \frac{1}{C(R+r_c)}} \approx \frac{\omega_0}{RC} = \frac{RC}{\sqrt{LC}} \times \frac{V_{IN}}{V_O} = R\sqrt{\frac{C}{L}} \times \frac{V_{IN}}{V_O} \tag{4}$$

Through the above model, it can be seen that the transfer function of Boost DC/DC stage depends on the working status in the system's set mode (depending on D and load R). To design PID controller for Boost object, we can use methods of pattern suppression, Bode diagrams, experiments … These are traditional methods. These traditional control methods are suitable for systems operating in a state of low fluctuations of load as well as input/output variable values of voltage. For systems operating in the state of large fluctuations (D and R with large variation), it is necessary to have appropriate adaptive control solutions. In the case of using the pattern suppression method, we can choose PID controller with the form:

$$PID(s) = \frac{D(s)}{E(s)} = K\frac{\frac{1}{\omega_0^2}s^2 + \frac{1}{\omega_0 Q}s + 1}{s} \tag{5}$$

Then:

$$K_p = \frac{K}{\omega_0 Q};\ K_i = K;\ K_d = \frac{K}{\omega_0^2} \tag{6}$$

The open loop transfer function of Boost DC/DC stage when using the PID controller follows the pattern suppression method as in formula (7).

$$G_H(s) = G_{do}K\frac{(1 + r_cCs)\left(1 - \frac{L}{R}\left(\frac{V_O}{V_{IN}}\right)^2 s\right)}{s} \tag{7}$$

The closed loop transfer function has the following formula (8):

$$G_k(s) = \frac{G_{do}K(1 + r_cCs)\left(1 - \frac{L}{R}\left(\frac{V_O}{V_{IN}}\right)^2 s\right)}{s + G_{do}K(1 + r_cCs)\left(1 - \frac{L}{R}\left(\frac{V_O}{V_{IN}}\right)^2 s\right)} \tag{8}$$

K can be selected so that the closed system has the pole point at the desired position. When the closed system have have un-desired zero points, we can also use sensible filters to eliminate these zero points.

### 2.2 Single-Phase SVPWM Inverter

The SVPWM inverter [2] acts as stage to convert the power from DC to AC. From the control point of view, it can be considered that the amplification stage has a factor of 1 (under voltage perspective) when the pulse hashing frequency is large enough. Technologically, this is the unit that performs the inverter vector modulation, power amplification, control circuit isolation and dynamic circuit.

The diagram of single-phase bridge voltage inverter is shown in Fig. 3 including 4 fully control valves V1, V2, V3, V4 and negative Diodes D1, D2, D3, D4. The negative diodes of the voltage inverter diagrams help the process of exchanging reactive power between the load and the source. The DC input is a voltage source with a characteristic of capacitor C with a value sufficiently large. Capacitor C serves both as a voltage balancing filter capacitor in case E source is a rectifier, and also has a role of reactive power storage exchanged with the load through negative Diodes.

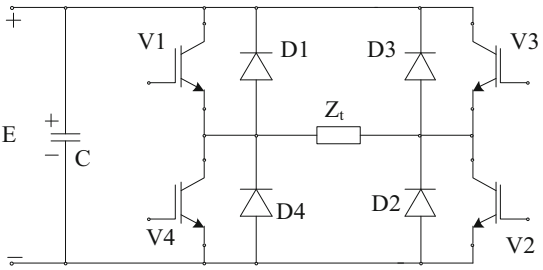


**Fig. 3.** Half-bridge voltage source inverter

## 3 Maximum Power Sticking Control Algorithm

Maximum Power Point Tracker (MPPT) is responsible for finding the working point of the panel array so that the maximum power received is corresponding to each given temperature and light intensity (MPPT point). To determine the MPPT point, two methods can be used: INC (Incremental Conductance); or P&O (Perturbation and Observe) [15, 16].

The P&O method is a simple and heavily used method thanks to the algorithm's simplicity and ease of implementation. However, when weather conditions change, this algorithm will become slower to follow the MPPT point. This method also has the disadvantage of not accurately identifying MPPT when the weather changes quickly, not suitable for frequent and sudden changes in weather conditions.

For the INC method [17]:

INC method is a type of MPPT algorithm. This method utilizes the incremental conductance (dI/dV) of the photovoltaic array to compute the sign of the change in power with respect to voltage (dP/dV). INC method provides rapid MPP tracking even in rapidly changing irradiation conditions with higher accuracy than the Perturb and observe method.

The input signal is the signal of voltage and current of solar panel array V_PV, I_PV; The output signal is the control signal D that controls the opening angle of the IGBT (Insulated Gate Bipolar Transistor) to get the maximum power. This method uses the total conductive power of the panel array to find the maximum power point as shown in Fig. 4. This method is based on the feature: The slope of the panel characteristic line is zero at the MPPT point, this slope is positive when on left of MPPT point, negative when on right of MPMP point.

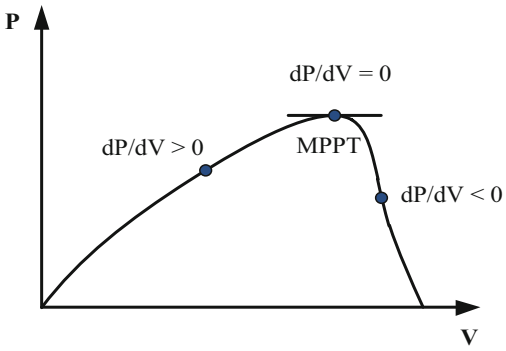


**Fig. 4.** Incremental Conductance method

Since $dP/dV = d(IV)/dV = I + V*(\Delta I/\Delta V)$:

$\Delta I/\Delta V = -(I/V)$: at MPPT point

$\Delta I/\Delta V > -(I/V)$: on the left of the MPPT point

$\Delta I/\Delta V < -(I/V)$: on the right of MPPT point

By comparing the instantaneous conductive value (I/V) with the incremental inductance value ($\Delta I/\Delta V$), this algorithm will find the maximum power operating point. At the MPPT point, the standard voltage $V_{ref} = V_{MPPT}$. Every time the MPPT point is detected, panel operation is maintained at this point unless there is a change in the current $\Delta I$, a change of current $\Delta I$ indicates a change of condition of weather and MPPT point. However, when the incremental inductance is too large, it will cause the system to operate incorrectly at the MPPT point and will be oscillated. The INC algorithm controlled via the reference voltage $V_{ref}$ is shown in Fig. 5.

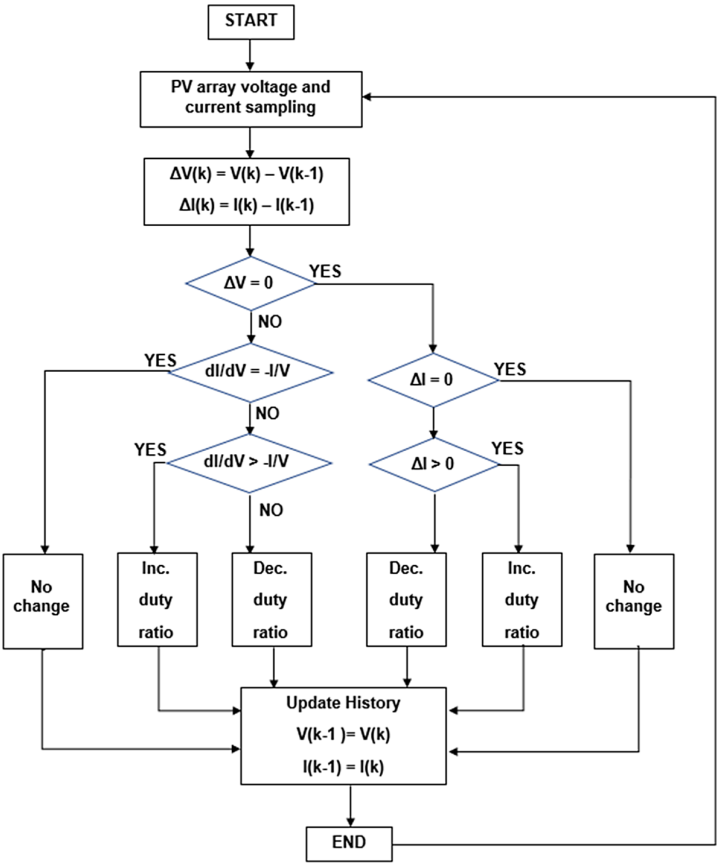


**Fig. 5.** INC algorithm controlled via $V_{ref}$ reference voltage [12]

## 4 Setting Up Simulation Model

### 4.1 Solar Panel Model

Simulation model of grid-connected solar power system in the form of DC bus is implemented on Matlab software. The power of the solar power calculated for the simulation is 1 kW. The output voltage of the system is 220 V and the frequency is 50 Hz. Solar panel model is set up as shown in Fig. 6.

The panel's input is light intensity and temperature. The output is voltage, direct current. The structure of a panel model is to use a function to control the current source. The function is written on M-file and embedded in the S-Function block.

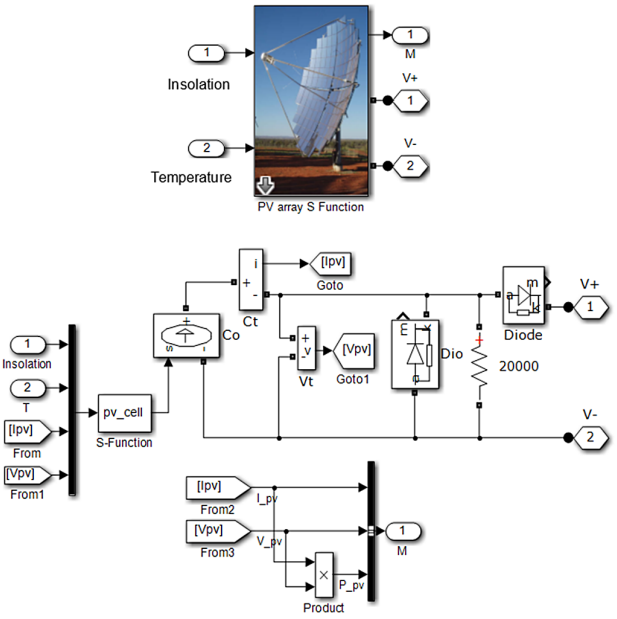


**Fig. 6.** Model of solar panel

## 4.2 DC/DC Power Converter Model

The model of DC/DC power converter is essentially a voltage BOOST unit as shown in Fig. 7. The model is built based on Matlab's powersim library. Parameters of the model are used to simulate: inductance L = 3 mH; 100 μF capacitor; power switching circuit using IGBT power semiconductor valve. Selected modulation frequency is 5 kHz. At the

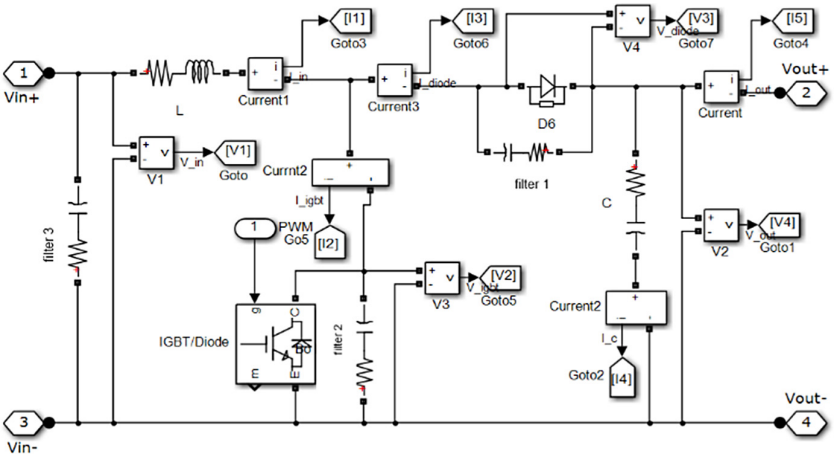


**Fig. 7.** Model of DC/DC voltage converter

points on the power circuit, both current and voltage sensor models are used to observe the time diagram of the current and voltage in the circuit.

### 4.3 Rectifier Stage

The rectifier stage uses a single-phase bridge rectifier circuit and does not use a filter capacitor because the quality of the single-phase bridge rectifier voltage is quite good. The connection between the two DC power circuits is shown in Fig. 8.

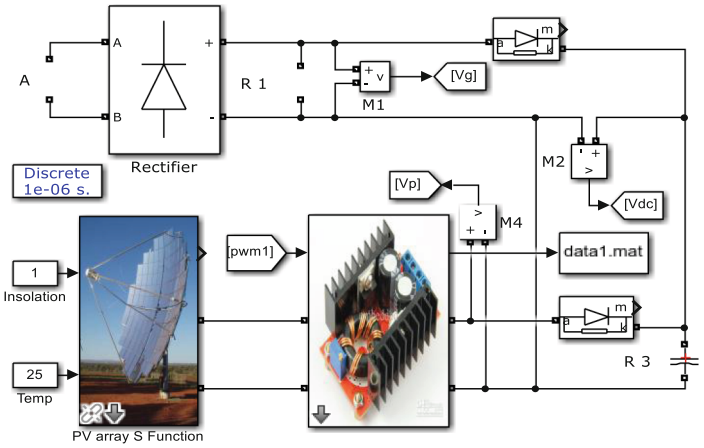


**Fig. 8.** DC power connection diagram

The principle of DC control ensures 2 requirements: 1) control the PV system to its maximum power; 2) the control ensures that the DC voltage of the PV power stage is always greater than the DC voltage at the output of the rectifier.

### 4.4 Two-Level Single-Phase Inverter Model

Single-phase inverter stage uses a two-level single-phase inverter with 4 IGBT valves as shown in Fig. 9. The sensor stage is for the purpose of measuring current and single-phase voltage on the power circuit. The modulation part uses SVPWM vector modulation technology with a 5 kHz pulse hashing frequency. The parameters used for modulation are Us amplitude and phase angle. Amplitude Us = 1 (reaches the maximum value to minimize harmonics). Phase angle is with cycle T = 20 ms.

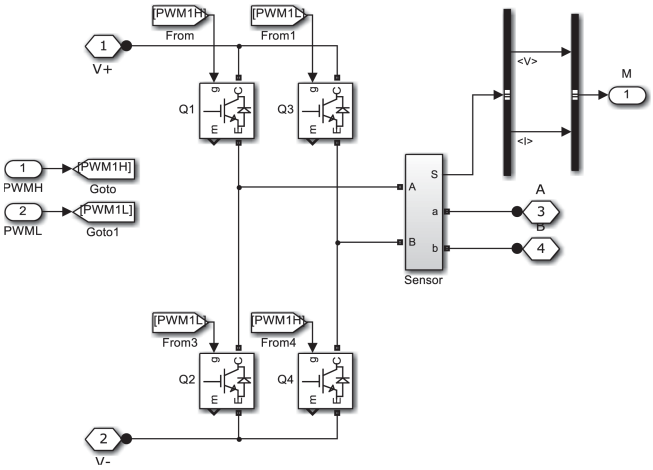


**Fig. 9.** H bridge single-phase inverter model

## 4.5 LCL Filter Model

The LC filter has a high-order harmonic removal function (described in Fig. 10). L1 and L2 inductors both select the value 1mH and filter capacitors have the value 2.2 μF.

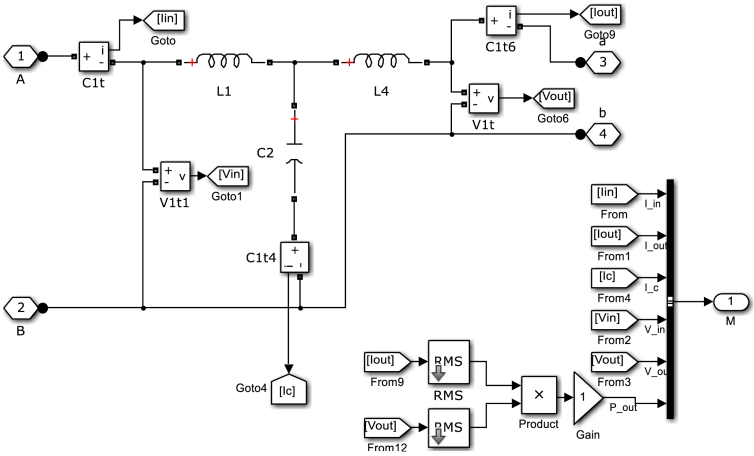


**Fig. 10.** LCL power filter diagram

## 4.6 Controller

PID unit model is as shown in Fig. 11.

PID controller is with signal set as the DC voltage supplied by the network plus an amount dV = 5 V and the feedback signal is a single-phase bridge rectifier voltage on

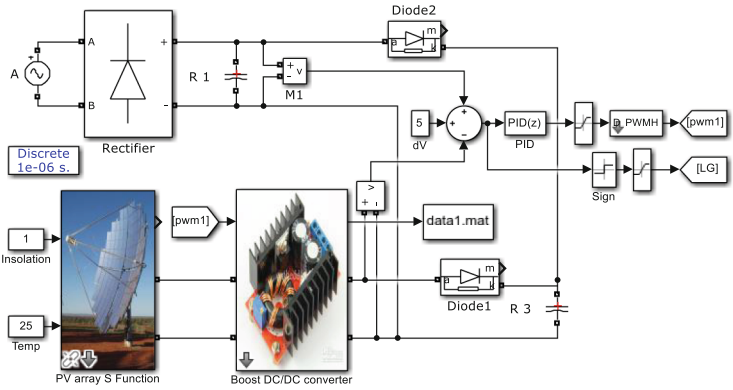


**Fig. 11.** PID controller

the load. In practice, this stage will use a single-phase voltage reduction transformer or specialized sensors to measure high DC voltage directly (not a voltage reduction transformer).

## 5 Simulation Results

### 5.1 Simulation of PV Panel Properties

The simulation of PV matrix properties from the library built on Matlab/Simulink applies to solar panels with the following specifications: Maximum power $P_{max} = 110$ W; Open circuit voltage $V_{OC} = 21{,}99$ V; Short-circuit current $I_{SC} = 6{,}72$ A; Voltage at maximum power $V_{mp} = 17{,}53$ V; Current at maximum power $I_{mp} = 6{,}28$ A; Panel performance 15.4% (Fig. 12).

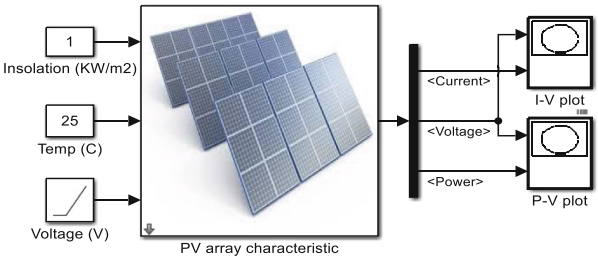


**Fig. 12.** Simulation diagram of PV panel

Characteristics IV and PV depend on the temperature and light intensity shown in Figs. 13, 14, 15 and 16. From the above characteristics, it can be seen that the working point with maximum power is always moving and depending on temperature as well as light intensity. At the high temperature, the power will decrease and at low temperature, the power will increase. For light intensity when the intensity is large, the power will be large and vice versa. Comparing the shape of the IV and PV characteristics obtained from the construction library with the characteristics I-V and P-V in documents [1–5], it is found that the results of building the PV matrix library above are completely appropriate.

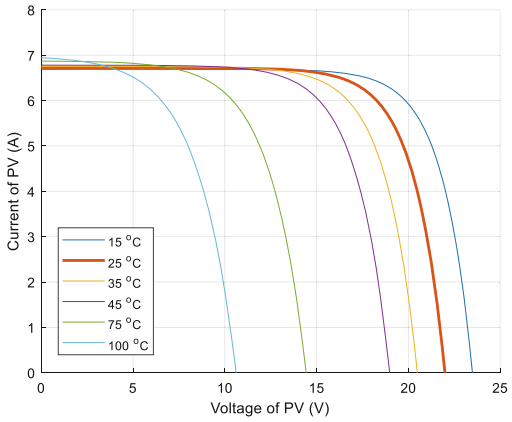


**Fig. 13.** I-V characteristics dependent on temperature at 1 kW/m$^2$ light intensity

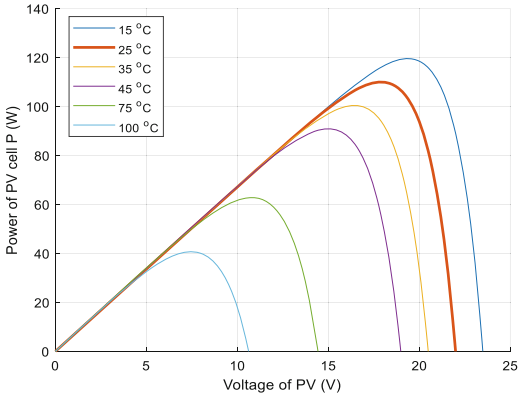


**Fig. 14.** P-V characteristic depending on temperature at 1 kW/m$^2$ light intensity

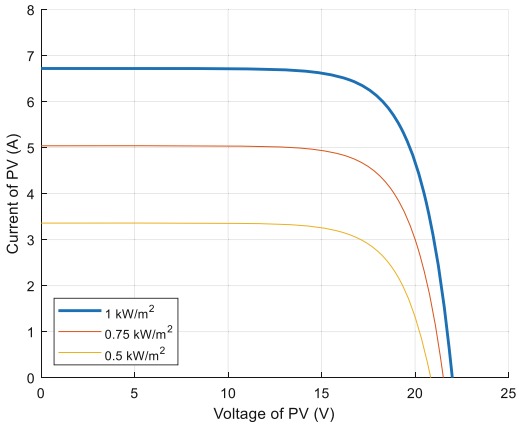


**Fig. 15.** I-V characteristic according to light intensity at 25 °C

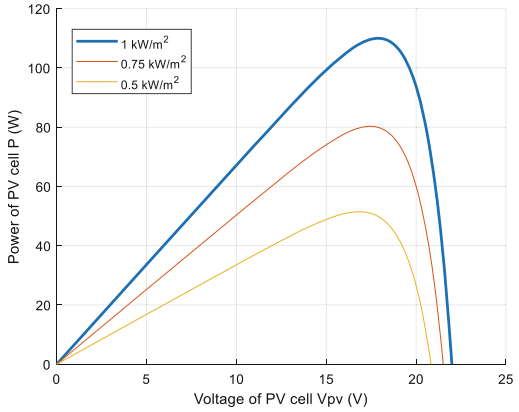


**Fig. 16.** P-V characteristic depending on the light intensity at 25 °C

### 5.2 Simulation of System Characteristics

Simulation system is with load R = 50 Ω. When the light intensity is as shown in Fig. 17a and the temperature is constant 25 °C. The DC response at DC bus grid points is given in Fig. 17b.

From Fig. 17, it can be seen: 1) the DC voltage on the PV side ($V_{DC}$) is controlled according to the DC side voltage ($V_g$); 2) when the PV power source is not sufficient for the load, the DC side voltage is connected to the DC BUS system and the DC voltage on the PV side falls into non-conduction state. This is the mechanism and principle of connecting DC-BUS grid in the system.

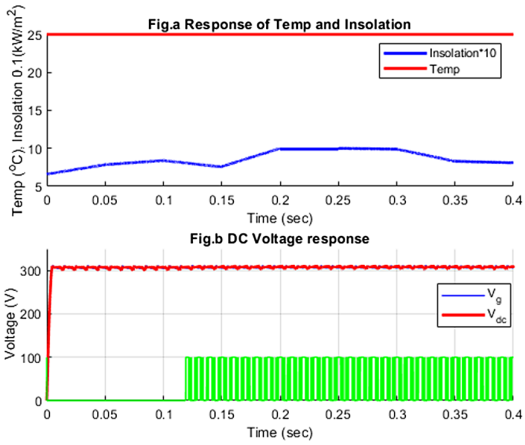


**Fig. 17.** DC voltage response at the stages

*A. Simulation of Boost DC/DC Unit's Characteristics* The current and voltage characteristics of the Boost DC/DC stage are shown in Fig. 18a.

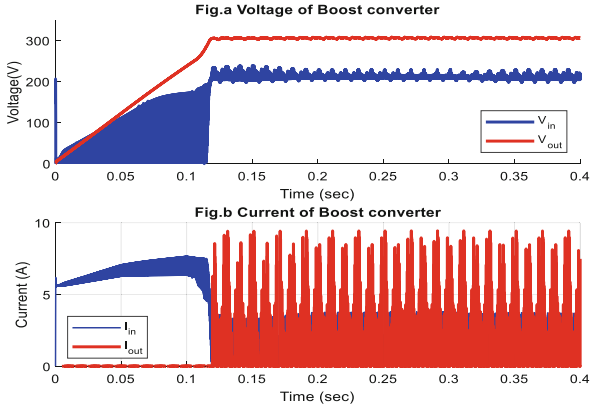


**Fig. 18.** Input/output current characteristics of Boost DC/DC stage

It can be seen that the time response (current and voltage) of Boost DC/DC stage has a pulse shape with the same frequency as the SVPWM modulation frequency at the control part. The interruption of the Boost DC/DC output current in Fig. 18b shows the DC-BUS separation of the Boost part. At this time, the energy from the rectifier will be fed to the inverter.

*B. Investigation of Phase-to-Phase Inverter Characteristics SVPWM* The phase voltage before filtering at the output of the SVPWM inverter is shown in Fig. 19a. To reduce harmonics, an additional LC or LCL power filter is required. Figure 19b is the wire voltage diagram of the inverter after the power filter. Properly calculating to select

the filter and the pulse hash frequency will produce a high quality sinusoidal signal while reducing the power valve switching losses. Figure 19b shows the wire voltage when the modulation frequency is 5 kHz, resistive load Y, value 50Ω, LCL filter with 1 mH, 2.2 μF and 1 mH values.

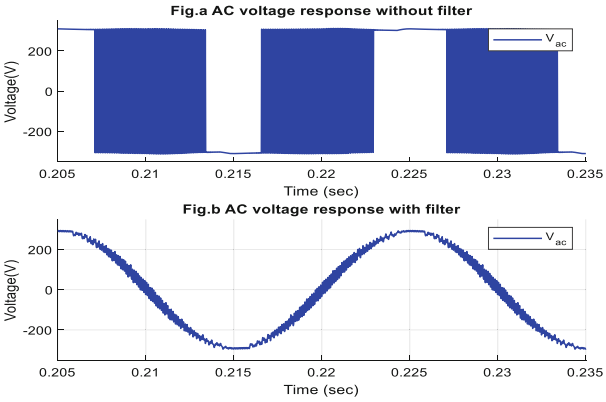


**Fig. 19.** Voltage diagram of the inverter before filtering

*C. System Performance* The performance of the system consists of 3 parts: performance of the rectifier, the DC/DC Boost DC unit and the single phase inverter. Note that the performance of the inverter has the performance of SVPWM modulation stage and the performance of the power filter stage. The simulation results show that the performance of rectifiers, boost units and inverters is 98%, 86% and 95%, respectively. Thereby leading to the performance of the whole system which reaches about 80%. Figure 20 simulates the performance from time to time of the power stages and the whole system.

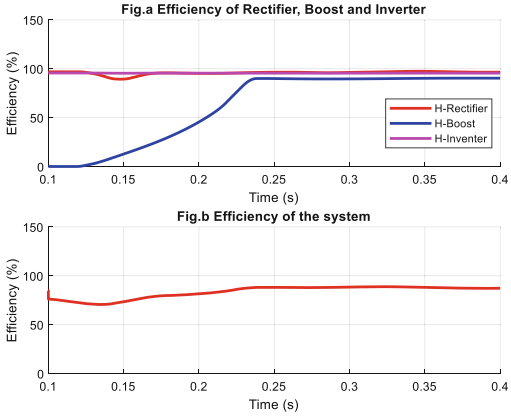


**Fig. 20.** System performance

We see that before 0.126 s, the performance of the Boost DC/DC unit is 0%. The reason is that this time the energy from PV is in the charging stage of Boost DC/DC stage and therefore, the PV source is not supplying to DC-BUS. In order to improve the performance of the system, it is necessary to focus on improving the performance of the Boost DC/DC stage, this is the stage with the lowest performance and the biggest impact on the performance of the system.

*D. Impacts of Modulation Frequency on the Performance of the Variable Stages*
To investigate the impacts of the pulse hashing frequency and the pulse width modulation on the performance of the Boost DC/DC, set the system with the following parameters: Light intensity: 1 kW/m$^2$; Temperature on PV: 25 °C; Voltage hashing frequency at Boost DC/DC stage (f-kHz): 2 kHz; 4 kHz; 6 kHz; 8 kHz; 10 kHz; 12 kHz; 14 Hz; 16 Hz; 18 Hz; 20 Hz; 22 Hz; 24 Hz; 26 Hz; 28 Hz; load value: 150Ω. Simulation results are shown in Table 1 and Fig. 21.

**Table 1.** BOOST DC/DC unit performance

| F (kHz) | The pulse width modulation D | | | | | | | | |
|---|---|---|---|---|---|---|---|---|---|
| | 0.1 | 0.2 | 0.3 | 0.4 | 0.5 | 0.6 | 0.7 | 0.8 | 0.9 |
| 6 | 63.35 | 57.67 | 51.09 | 50.11 | 49.32 | 48.37 | 48.47 | 46.63 | 41.50 |
| 8 | 78.57 | 66.34 | 64.79 | 60.75 | 57.73 | 56.57 | 52.84 | 51.13 | 47.16 |
| 10 | 88.77 | 75.43 | 67.88 | 62.17 | 58.10 | 57.14 | 52.47 | 53.93 | 48.26 |
| 12 | 92.39 | 83.95 | 79.34 | 74.36 | 63.40 | 58.73 | 53.30 | 54.99 | 51.32 |
| 14 | 93.06 | 87.06 | 83.76 | 79.46 | 67.44 | 61.45 | 54.85 | 54.23 | 55.46 |
| 16 | **93.12** | 88.49 | 85.84 | 83.81 | 71.71 | 67.44 | 55.91 | 55.69 | 56.85 |
| 18 | 92.70 | **88.96** | 86.77 | 85.30 | 74.58 | 67.89 | 56.72 | 57.52 | 56.04 |
| 20 | 92.12 | 88.88 | 86.90 | **85.78** | 76.82 | 67.92 | 57.18 | 58.42 | 56.50 |
| 22 | 91.21 | 88.46 | **86.92** | 85.68 | 77.07 | 67.63 | 57.99 | 60.29 | 57.30 |
| 24 | 90.31 | 87.86 | 86.29 | 85.28 | 77.27 | 68.12 | 64.56 | 59.97 | 58.31 |
| 26 | 89.34 | 87.10 | 85.63 | 84.64 | **79.90** | **76.42** | 68.19 | 63.44 | 60.93 |
| 28 | 88.15 | 86.27 | 84.96 | 83.93 | 79.64 | 75.62 | **70.83** | **67.64** | **61.82** |

From the results in Fig. 21, it can be seen: Boost stage performance depends greatly on the pulse hashing frequency and the width of the voltage hashing pulse. Increasing the width of the voltage hashing pulse width will reduce the system performance. The pulse hashing frequency also needs to be selected appropriately. If this value is too large, it will cause losses on the IGBT protection RC circuits and the valve ON/OFF valve power will increase, resulting in a decrease in performance. However, if the pulse hash frequency is not large enough, the quality of the DC voltage in the circuit will not be high. Therefore, the design process needs to select the frequency of the voltage hashing pulse and the scope of adjusting the pulse width appropriately for the system to achieve high performance.

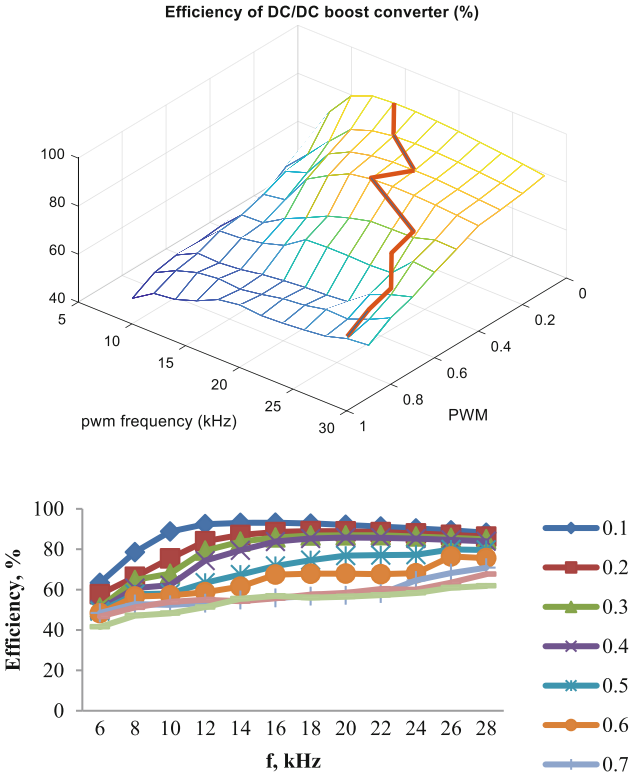


**Fig. 21.** System performance depending on the frequency and width of the voltage hashing pulse width

With the simulation results, it is recommended to select the working area D = 0–0.4 and the pulse hash frequency range 16–22 kHz to achieve the highest possible performance. In the case where a large modulation range (D with a large range of values) must be used, a functional structure that automatically adjusts the pulse hashing frequency so that the system will achieve the highest possible performance.

## 6 Conclusion

From the results of model building, control algorithm and simulation of the grid-connected solar power system at the DC-BUS stage, the system operates stably, ensures the requirements of DC-BUS grid. For the above system, we can realize some advantages as follows:

– The system operates safely because it does not have to handle the oasis phenomenon as in the AC grid system.
– Control structure and algorithm are simple, easy to adjust and execute

– The modulation part of SVPWM does not need to implement the algorithm to stick to the grid.

In order to improve converter performance further, in the coming time, we will:

1. Research, develop and test the real system based on embedded system platform to get the most accurate evaluation results on grid-connected solar power system at DC-BUS stage.
2. Implement a self-tuning mechanism of voltage hash frequency based on the modulation pulse width in order to maximize the system performance.

**Acknowledgements.** The authors wish to thank the Institute of Energy Science (IES) and Vietnam Academy of Science and Technology (VAST) for their support to the research activity of Project "Research on completing the technology, constructing and transferring the model of exploiting and proper using solar and wind energy for production and daily living in Central Highland", TN17/C03.

## References

1. Chuong, T.T.: Voltage stability analysis of grids connected wind generators. In: The International Conference on Electrical Engineering, No. O-054 (2008). Article No. 1
2. Minh, N.D., Van Huy, B., Quan, N.T., Ninh, N.Q., Chuong, T.T.: Research and Design of Grid-Connected Inverter in Photovoltaic System With Svpwm Technique. Int. J. Eng. Technol. Manag. Res. 6(11), 18–31 (2020)
3. Amaral, G., et al.: Control in Power Electronics, vol. 369, no. 1. (2013)
4. Patil, U., Kolte, D.M.: Simulation of DC-DC Boost Converter for SPVM (2015)
5. de Cesare, G., Caputo, D., Nascetti, A.: Maximum power point tracker for portable photovoltaic systems with resistive-like load. Sol. Energy **80**(8), 982–988 (2006)
6. Arathy, M., Sreekala, P.: Design and implementation of A PV powered five level inverter using multilevel differential boost converter. Int. J. Adv. Res. Electr. Electron. Instrum. Eng. **3**(2320 – 3765), 10315–10320 (2014)
7. Pal, S., Dalapati, S.: Digital simulation of two level inverter based on space vector pulse width modulation. Indian J. Sci. Technol. **5**(4), 2557–2568 (2012)
8. Anand, R., Gnanambal, I.: Modeling and analysis of cascade multilevel DC-DC boost converter topologies based on H-bridge switched inductor. Res. J. Appl. Sci. Eng. Technol. **9**(3), 145–157 (2015)
9. Rasheed, M., Omar, R., Sabari, A., Sulaiman, M.: Validation of a three-phase cascaded multilevel inverter based on Newton Raphson (N.R.). Indian J. Sci. Technol. **9**(20), 1–13 (2016)
10. Omar, R., Rasheed, M., Sulaiman, M., Tamijis, M.R.: Modeling and simulation of a three phase multilevel inverter for harmonic reduction based on modified space vector pulse width modulation (SVPWM). J. Theor. Appl. Inf. Technol. **77**(2), 178–189 (2015)
11. Stepins, D., Huang, J.: Effects of switching frequency modulation on input power quality of boost power factor correction converter. Int. J. Power Electron. Drive Syst. **8**(2), 882–899 (2017)
12. Eichhorn, T.: Boost converter efficiency through accurate calculations. Power Electron. Technol. **34**(9), 30–35 (2008)

13. Hauke, B.: Basic Calculation of a Boost Converter's Power Stage. Texas Instruments. Application Report November November 2009, pp. 1–9 (2009)
14. Quang, N.P.,Gmbh, E.: Inverter control with space vector modulation. Power Syst. **20**, 17–59 (2008)
15. Ahmed, J., Salam, Z.: An improved perturb and observe (P&O) maximum power point tracking (MPPT) algorithm for higher efficiency. Appl. Energy **150**, 97–108 (2015)
16. Kumar, A.: Overview of genetic algorithm technique for maximum power point tracking (MPPT) of solar PV system. no. Cognition, pp. 21–24 (2015)
17. Liu, F., Duan, S., Liu, F., Liu, B., Kang, Y.: A variable step size INC MPPT method for PV systems. IEEE Trans. Ind. Electron. 55(7), 2622–2628 (2008)